Astron. Astrophys. 283, 805–812 (1994)

ASTRONOMY AND ASTROPHYSICS

Integrated spectral properties of star clusters in the near-ultraviolet***

E. Bica[1], D. Alloin[2], and H.R. Schmitt[1]

[1] Departamento de Astronomia, IF-UFRGS, CP,15051, CEP,91501-970, Porto Alegre, RS, Brazil
[2] Observatoire de Paris, URA173 CNRS, F-92195 Meudon Principal Cedex, France

Received 11 August 1993 / Accepted 27 September 1993

Abstract. We study integrated spectra of 37 star clusters in the range 3100 – 4200 Å . The sample includes Galactic globular and open clusters, as well as Magellanic Cloud clusters. Feature equivalent widths (W) and continuum distribution are analyzed as a function of age and metallicity. In particular we discuss the behaviour of the Balmer Jump and of the 4000 Å Break, which are measured by the same continuum ratio $C3660$ Å / $C4020$ Å . For ages $t < 500$ Myr the Balmer Jump is dominant over the 4000 Å Break and for $t < 50$ Myr it is an excellent age discriminator. The effects of blue Horizontal Branch morphology on globular cluster spectra are also discussed: they increase the Balmer line W, but do not dilute substantially the Near-UV metallic features. The present data will provide a means to connect optical to UV integrated star cluster spectra, with important applications in stellar population analyses, in particular for distant galaxies at redshift up to 1.

Key words: globular clusters – open clusters – galaxies: star clusters – Magellanic Clouds – ultraviolet: stars – galaxies: evolution

1. Introduction

The analysis of composite stellar populations where star formation has occurred at different epochs requires that both age and metallicity be considered as essential parameters. A high star formation rate goes with a high metallicity enrichment, as was the case of stellar populations at the center of giant elliptical galaxies. It should be noticed also that galaxies are not isolated objects, and that phenomena such as interactions and mergers may provide fresh gas for further nuclear star formation, either from other parts of the galaxy or from outside. This can have important implications on the study of the Galactic bulge, abundances of heavy elements in nuclear HII regions, abundance gradients in the disc of spiral galaxies (see for a review e.g. Pagel & Edmunds 1981; Frogel 1988, 1992 and Shields 1990).

In order to interpret galaxy spectra, we have developed a population synthesis method, using a base of star clusters and a grid of their integrated spectral properties over the range 3700—10000 Å, parametrized with age and metallicity (Bica 1988 and references therein). In the latter synthesis of galaxy spectra, a well-focused solution requires observations of the base star clusters in the spectral range where they mostly emit. In other words, the red composite population at the heart of massive elliptical galaxies was recovered with accuracy, as the constraints we use presently, distributed over the range 3700—10000 Å, are appropriate to the light dominant components in these objects. On the other hand, the analyses of blue composite populations were subject to a larger uncertainty: the light-dominant components would be better characterized by spectral features in the ultraviolet range (Schmidt et al. 1991). This led us to build, in the present paper, an extension of the grid of star cluster integrated spectral properties to the Near-UltraViolet (NUV) range.

The NUV spectra of star clusters are also important in the synthesis of high redshift galaxies (Jablonka et al. 1990).

Modern detector spectroscopy studies in the NUV range are relatively scarce as compared to the amount of observations available at longer wavelengths. Gunn & Stryker's (1983) stellar library reaches the ultraviolet atmospheric limit. Cullum et al. (1985) explained the methods and composition of the mixture used to coat CCDs and presented the observations of the Seyfert 1 galaxy NGC3783 and the central star of the planetary nebula NGC5882 in the spectral range 3100–4500 Å. Carbon et al. (1987) analyzed 83 stars in the solar neighborhood in the range 3100–5100 Å. Boulade et al. (1988) studied the nucleus of M32 and 60 field stars covering a range in temperature, luminosity and metallicity. Davidge et al. (1990) discussed the NH 3360 Å feature in the central regions of M31 and M32.

In the present paper we provide NUV integrated star cluster spectra for a cluster sample already discussed in the visible and near-infrared ranges (Bica & Alloin 1986a,b 1987; hereafter

Send offprint requests to: D. Alloin

* Based on data collected at the European Southern Observatory, La Silla, Chile.

** Tables 1,2,3 are only available in electronic form: see the editorial in A&A 1992, Vol. 266 No 2, page E1

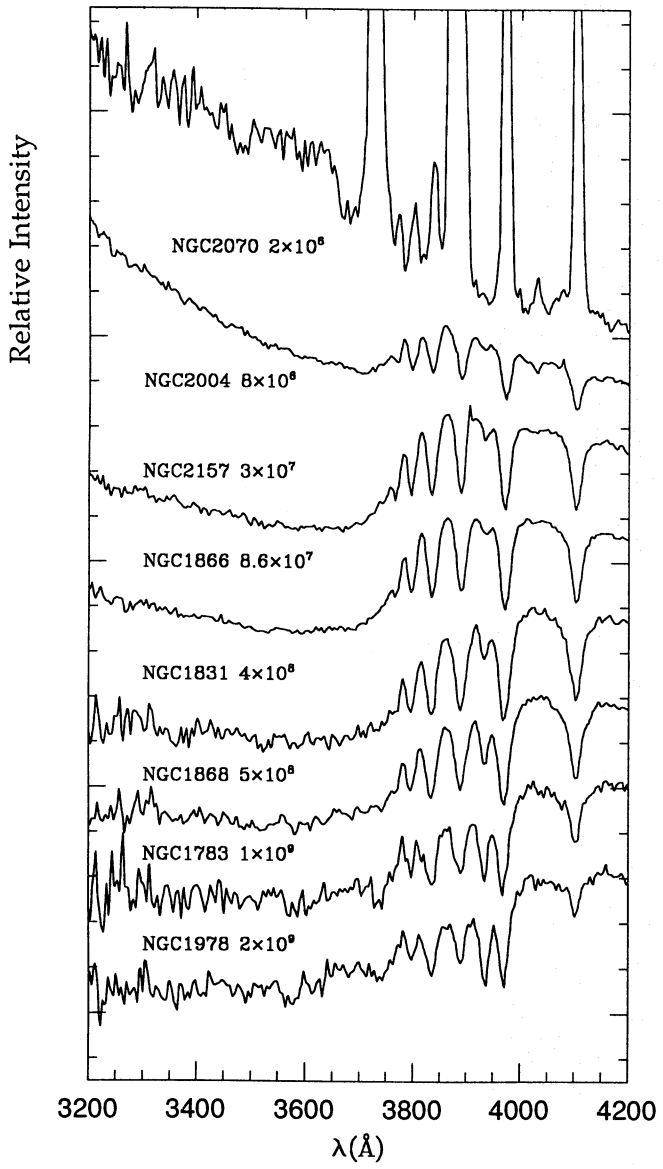

Fig. 1a. Representative spectra of young and intermediate age (increasing from top to bottom) star clusters. The relative intensity spectra are normalized at 4020Å and for clarity, constants are added. Ages in years are indicated

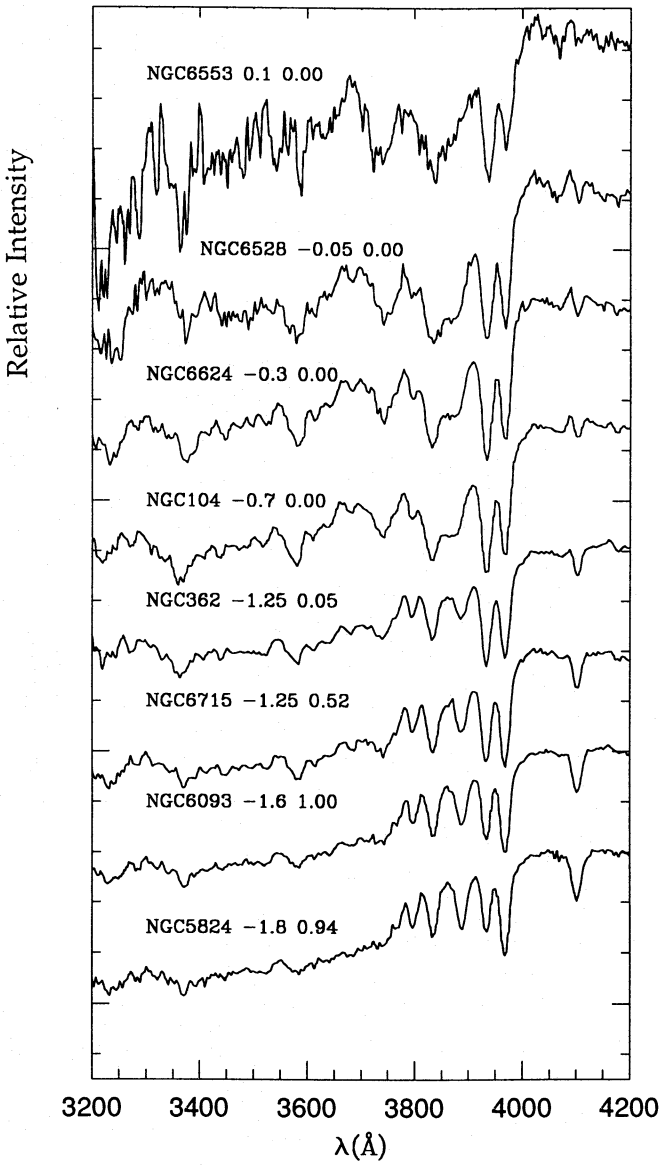

Fig. 1b. Representative spectra of globular clusters of different metallicities (increasing from bottom to top). Normalization and constants as in Fig. 1a. Metallicity and Horizontal Branch morphology parameter are indicated

BA86a,b and BA87). We describe the observing procedure and data reduction in Sect. 2. In Sect. 3 we define the windows and continuum points in the NUV and present the measurements. We also make comparisons with the spectral region in common with BA86a. In Sect. 4 we discuss the equivalent width results, the Balmer Jump and the 4000Å Break as a function of age and metallicity and point out which features are the most useful discriminators. We also discuss the influence of the Horizontal-Branch morphology on the NUV spectra of globular clusters. In Sect. 5 we summarize the conclusions of this work and point out prospective applications of the present study.

2. The data

2.1. The sample

In essence, we study the behaviour of absorption features in integrated spectra of star clusters for which metallicity and age were known from previous studies in the literature. The star cluster sample spans approximately the same age and metallicity ranges as those studied in the visible and near-infrared ranges (BA86a, BA87). The observed objects are listed in Table 1 (accessible in electronic form), together with age and metallicity values, as well as foreground reddening E(B–V) and the Mironov Horizontal Branch morphology parameter B/(B+R) for the old clusters. The data were compiled in BA86a, except updated and new ones, as indicated in the table. The sample includes 21 globular

clusters and 3 open clusters in the Galaxy and 11 LMC and 2 SMC star clusters. We adopt a globular cluster age of 15 Gyr. The metallicity scale of metal rich globular clusters is still a matter of debate, which will only be solved through a considerable observational and theoretical effort, by means of high dispersion spectroscopy of individual giants , better opacities in model atmospheres and a more complete set of atomic and molecular parameters in spectral models. The main objective of this sample was to span wide ranges in age and metallicity with a mesh of points as dense as possible. This should allow one to interpolate spectral properties in order to construct a grid at suitable steps in age and metallicity.

2.2. *The observations and reductions*

The observations were carried out in two runs, January 1988 and July 1989, with the Boller & Chivens spectrograph at the Cassegrain focus of the 2.2 m and the 1.52 m telescopes at the European Southern Observatory (ESO), La Silla, Chile. We employed coated GEC CCDs, ESO CCD #7 and ESO CCD #14, in the first and second runs respectively. The CCDs have 576x385 pixels of size 22x22 μm. The slit length covered about two thirds of the CCD width and was oriented along the East–West direction. The slit widths were 4″(1988) and 5″(1989). The gratings used were ESO #2 with 224 Å mm^{-1} (1988) and ESO #8 with 193 Å mm^{-1} (1989). Helium and Argon comparison lamps for wavelength calibration and dome flat fields were used. The spectral resolution as measured from comparison lamp lines is $\approx$ 15Å in both runs. The spectral ranges covered 3000–5600Å (1988) and 3000–5200 Å (1989). The standard stars observed were Fei24 and Fei66 (1988), and EG274 and Fei110 (1989).

The star clusters were scanned along the North-South direction for a better sampling of their stellar content. The background sky was taken either in the same frame or in a separate one, depending on the cluster size.

The reductions were carried out in a standard way for CCD observations using the IHAP system at ESO Garching.

3. The spectra

The spectral analysis was made with the SPEED package at the Instituto de Física/UFRGS computer center in Porto Alegre. The cluster spectra were reddening corrected with the normal Galactic reddening law (Seaton 1979) and foreground E(B–V) values from Table 1. The spectra were redshift corrected using values from the literature and/or measured in the spectra themselves. We illustrate in Fig. 1a spectra of young and intermediate age clusters in the LMC, and in Fig. 1b Galactic globular clusters of different metallicities. The most conspicuous features in the NUV are the Balmer Jump and the 4000Å Break. Both correspond to a sudden flux decrease in the range 3600–4000Å with respect to longer wavelengths. The 4000Å Break, which occurs preferentially in red population spectra, appears like a discontinuity close to 4000Å, mostly caused by the presence of the strong CaII lines H and K, together with CN bands and FeI lines. The Balmer Jump, which is more conspicuous in blue populations (old metal poor clusters and young clusters), is more spread in wavelength, corresponding to the accumulated blend of Balmer lines towards the Balmer limit (3646Å).

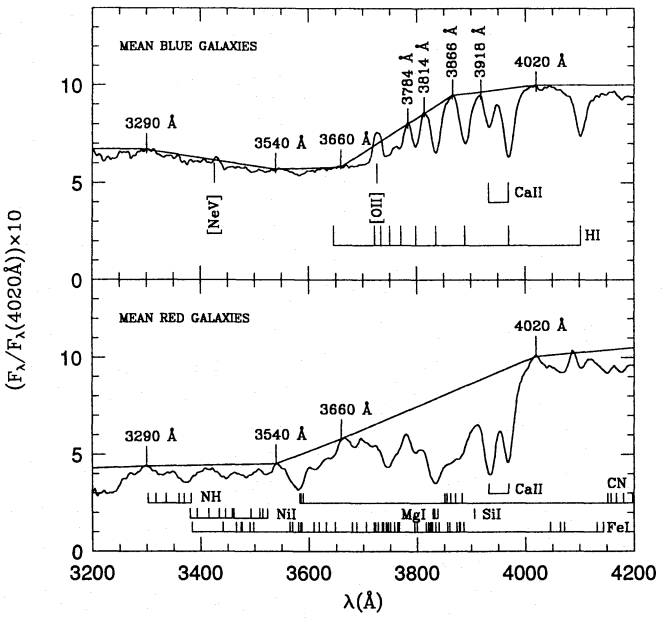

Fig. 2. Continuum tracing definition based on high S/N average spectra of blue (top) and red (bottom) galaxies. Continuum regions are labeled. The main absorbers in prominent features are indicated. In the upper spectrum the emission-lines [NeV]λ3426Å and [OII]λ3727Å are present

3.1. *Measurements*

Following BA86a and BA87 we adopted similar procedures to define a series of windows for continuum tracings, and windows for W's of spectral features in the NUV. The observing runs were partly devoted to star cluster observations and partly to galaxy observations. Therefore, we have collected at the same time spectra for a sample of 94 galaxies. Since our ultimate objective is synthesizing the composite stellar population of galaxies, we defined the spectral windows on very high signal to noise (S/N) average galaxy spectra for typically blue and red stellar populations. The average spectra are shown in Fig. 2, together with the adopted continuum points and tracings. The importance of adopting these average galaxy spectra for window definitions comes from the fact that their different redshift corrections, altogether cancel out eventual local detector problems. As we can see in Fig. 2 the continuum points were selected in order to be suitable simultaneously for blue and red populations. As pointed out in BA86a, in the region 3600—3900Å some additional continuum points are necessary in blue populations to take into account the spectral continuum shape near the Balmer Jump. The continuum windows (10—20Å wide) are centered at 3290Å, 3540Å, 3660Å and 4020Å. The supplementary points, which in some cases of blue populations are needed, are located at 3784Å, 3814Å, 3866Å and 3918Å.

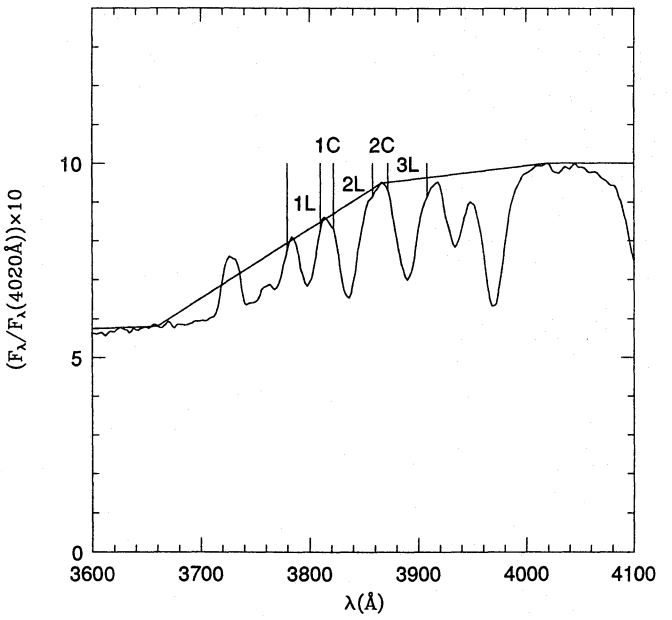

Fig. 3. Redefinition of windows in the range 3780-3908Å. Enlargement of the average spectrum of blue galaxies from Fig. 2. Continuum tracing and new windows are indicated

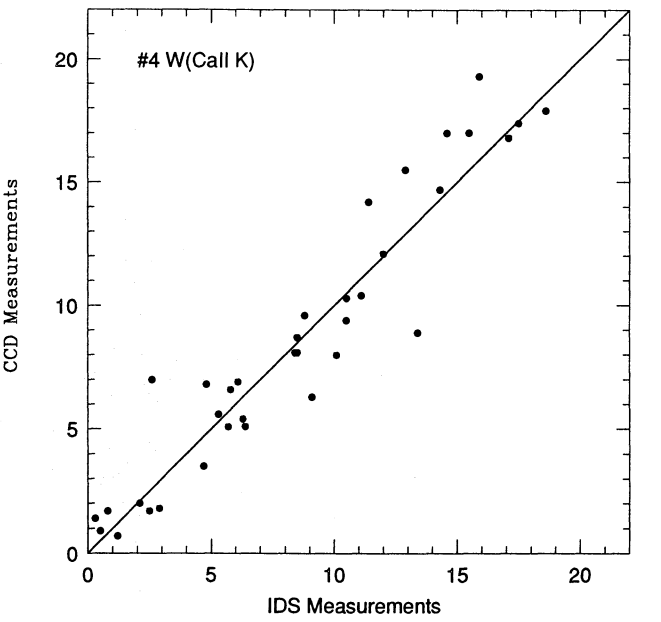

Fig. 4. Comparison of the CaII K equivalent widths from the present CCD data and from the IDS data in BA86a

The resulting new windows in the range 3290−3780 Å and corresponding main absorbers are listed in Table 2 (accessible in electronic form). Identifications of the main absorbers are also indicated in Fig. 2. They were searched in spectral atlases, line and molecular band identification tables, as well as in stellar spectra throughout the literature (e.g. Griffin 1968; Davis 1947; Pearse & Gaydon 1965; Faÿ et al. 1974). We also provide in Table 2 a redefinition of windows in the range 3780-3908Å with respect to BA86a. The previous windows #1, #2 and #3 are replaced by five new ones. They are shown in Fig. 3, on an enlargement of the average blue galaxy spectrum, together with the corresponding continuum tracing. Notice that they isolate three Balmer lines and two continuum regions in blue populations, whereas in red metal-rich ones (Fig. 2) the whole region corresponds to metallic absorption. This was done in order to disentangle such populations in future population syntheses.

We present the W's and continuum ratios for the star cluster sample in Table 3 (accessible in electronic form). We only show values for the most significant windows from Table 2. Typical errors on W, owing to continuum placement uncertainties and noise in the feature window, are $\sigma(W)$ ≈0.5Å, or ≈3% for strong lines and ≈15% for weaker ones. The continuum uncertainties are $\sigma(C)$ ≈2%.

3.2. Comparison with common windows in BA86a

Measurements of W for features in common between the present CCD observations and the IDS ones in BA86a,b were compared. In Fig. 4 we plot the CCD×IDS measurements for window #4 CaII K, where a good agreement is seen. The dispersion is within expectations of observational errors. We note that we used the continuum point λ ≈3660Å for the CCD spectra (Fig. 2), whereas that for the IDS spectra it was at λ ≈3720Å, owing to an observational cutoff. However this change has not affected significantly the W values. From similar comparisons we realized that for the IDS measurements of window #1 in BA86b, the uncertainties were quite large owing to instrumental border effects. In addition, the latter window is now split in two, in order to better explore the continuum region and Balmer line information in blue populations (Sect. 3.1).

4. Discussion

4.1. The NUV windows

We show in Figs. 5 and 6 a series of plots providing the W values for a number of features versus metallicity. Figure 5 deals with pure metallic features (metal atomic lines and/or molecular bands). We can see that these NUV metallic features behave like those in the blue spectral region (BA86a), i.e. old clusters have systematically larger W's whereas younger ones have diluted W's. However the dilution for NUV features is stronger than that observed in the visible range. In fact, the NUV dilution is so strong in young clusters that their W's are considerably smaller than those of the most metal-poor globular clusters. The shorter the wavelength the stronger the dilution is, such as in the NH feature (λ ≈3360Å). The dilution effect is due to the presence of hotter main sequence stars in younger clusters which contribute to the underlying continuum, but not to the features. An additional difference between features in the NUV and visible range, is that the oldest blue clusters NGC1831 and NGC1868 (ages 400 Myr and 500 Myr respectively), tend to behave like the intermediate age clusters (0.9<age(Gyr)<7). The reason why they are not much diluted in the NUV is because their turn-off corresponds to ≈A type stars, and consequently

their continua are stronger in the blue than in the NUV. Figure 6 presents windows which are a blend of Balmer lines with metallic features. The blue clusters, where the Balmer absorption lines peak in intensity, have relatively larger equivalent width values when compared to the pure metallic feature "g" (Fig. 5) at similar wavelength. The importance of this effect depends on the relative strength of Balmer and metallic absorptions: in the (CaII H+Hϵ) window "5" (Fig. 6), the metallic feature is stronger, whereas in window "k" the accumulation of Balmer lines dominates the absorption, and consequently young clusters merge with globular clusters in the plot. In window "1L" the Balmer line is important relative to the metallic absorption, while in window "2L" the Balmer line is weaker than the CN absorption, although in absolute values HI9 (window "2L") is stronger than HI10("1L").

Considering only globular clusters the slopes in the W vs metallicity plots are steeper for the pure metallic features (Fig. 5) than for windows containing Balmer lines (Fig. 6). This is due to blue Horizontal Branches in more metal poor clusters (Sect. 4.3).

We show in Fig. 7 window "2C", which in blue populations corresponds to the continuum adjacent to HI9 ("2L"), and in red metal-rich populations to CN absorption. In this plot we observe the maximum separation between old metal-rich populations and intermediate plus young age clusters. On the other hand metal poor globulars have a similar level of W values, when compared to those of young clusters, which was not the case for the metallic features in windows "b" (NH) and "g" (FeI,CN) in Fig. 5.

Comparing Figs. 5, 6 and 7 we notice that young, intermediate and old clusters, as well as metal poor and metal-rich ones can be disentangled, when we take into account the W behaviour in different windows simultaneously. These criteria can be used in a population synthesis algorithm.

The metallic features that we observe in the NUV arise mostly in cool stars, so the dilution effect caused by hot stars in young clusters precludes their direct use as metallicity indicators. On the other hand, farther away in the UV, the observed metallic features arise in the *hot stars* themselves. These features are from high ionization stages of heavy elements such as SiIV and CIV, as can be seen in IUE spectra of young clusters in the LMC (Cohen et al. 1984). Consequently the behaviour of metallic features in the 1000–2000Å range as a function of metallicity and age is expected to be different from that of metallic features in the NUV and blue-violet ranges.

4.2. Balmer jump and 4000Å break

As pointed out in Sect. 3, the dependence of the Balmer Jump and of the 4000Å Break on age and metallicity can be visualized in Figs. 1a and 1b. In fact, the spectral region 3650–4000Å reveals an intricate combination of metallicity and age effects. Among globular clusters (Fig. 1b) the Balmer Jump is important at low metallicities because of the presence of blue Horizontal Branch stars, whereas for the most metal-rich clusters like NGC6528 and NGC6553 an essentially pure 4000Å Break is observed. At intermediate and young ages (Fig. 1a) we also see the 4000Å Break and Balmer Jump varying. However in this case the main origin of the Balmer Jump is age, due to the increasingly more luminous and hotter turn-off in younger clusters. In the intermediate age clusters NGC1978 and NGC1783 (1 and 2 Gyr respectively) both effects are comparable. For younger ages the Balmer Jump is dominant and its strength varies considerably. For ages 30≤t(Myr)≤400 the Balmer Jump is very strong. In NGC2004(≈10 Myr) it becomes weaker, because the turn-off is much hotter. Finally, for an integrated HII region (NGC2070, Fig. 1a) the Balmer Jump is in emission. The latter spectrum is a combination of one from pure emission regions and another from the embedded central cluster, which reproduces the integrated W(Hβ) obtained photometrically by Dottori & Bica (1981). We show in Fig. 8 the individual spectra of the pure emission and of the essentially pure star cluster. Notice that in the former a strong Balmer Jump in emission is present, whereas in the latter it is absent, since the flux is dominated by O, B and WR stars (some nebular emission is also seen).

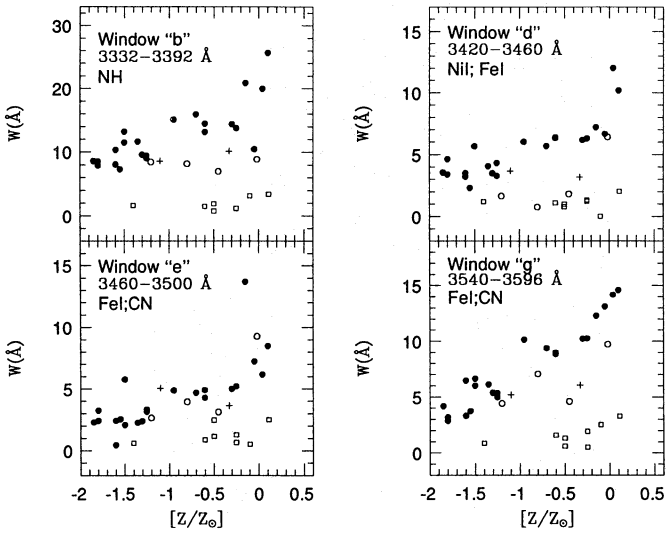

Fig. 5. Equivalent widths of pure metallic features as a function of metallicity, for a selection of four windows. Symbols indicate different age groups: open squares: 0<t(Myr)<300; plus sign 300<t(Myr)<800; open circles: 0.9<t(Gyr)<7; filled circles: globular cluster ages

We show in Figs. 9a and 9b the continuum ratio C3660Å/C4020Å (Table 3) as a function of age and metallicity, respectively. The ratio is a measure of the Balmer Jump and/or of the 4000Å Break and the continua are close enough in wavelength in order not to be much dependent on reddening. We can see in Fig. 9b that there is no correlation between this ratio and the metallicity, mostly because of the transition effects of the Balmer Jump to the 4000Å Break discussed above. For the same reasons there is no dependence of the ratio on age for t>50 Myr. On the other hand the ratio is an excellent discriminator for younger ages (C3660Å/C4020Å>0.70) in the sense that the Balmer Jump rapidly tends to disappear when the turn-off becomes hotter for the youngest clusters. Therefore this ratio is

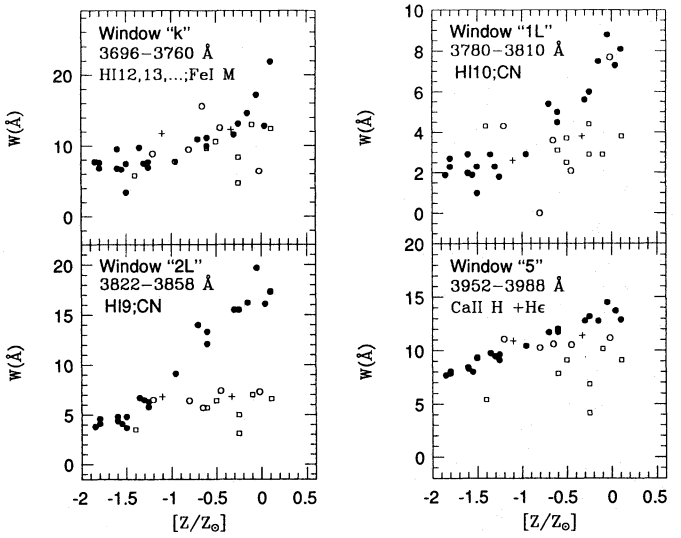

Fig. 6. Equivalent widths for windows containing Balmer lines. Symbols as in Fig. 5

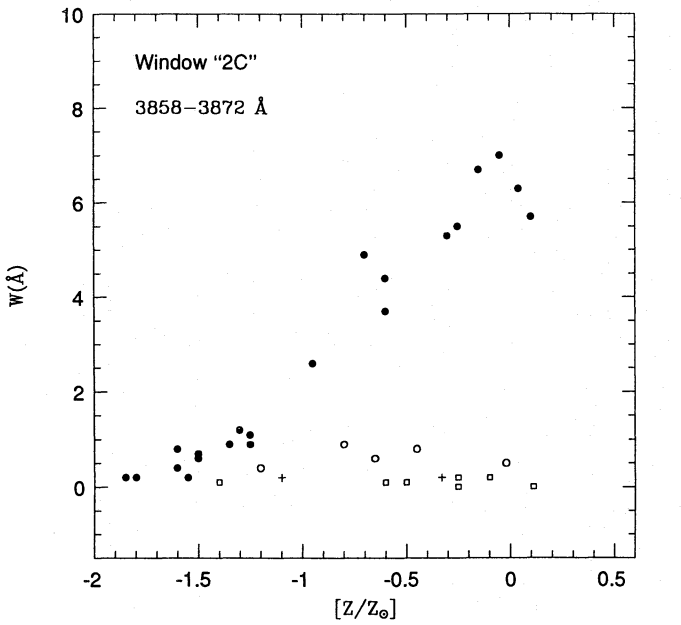

Fig. 7. Equivalent widths for a window which, in blue clusters corresponds to continuum and, in red clusters to CN absorption. Symbols as in Fig. 5

a good age indicator exactly in the interval where the Balmer lines become troublesome owing to emission contamination.

4.3. Horizontal branch morphology in globular clusters

The Horizontal Branch (HB) morphology in colour magnitude diagrams (CMD) of globular clusters is correlated with metallicity, in the sense that metal rich clusters present only red HBs, while for lower metallicities, HBs tend to be blue. There are clusters which deviate from this correlation, mostly intermediate metallicity globular clusters with red HBs, constituting the

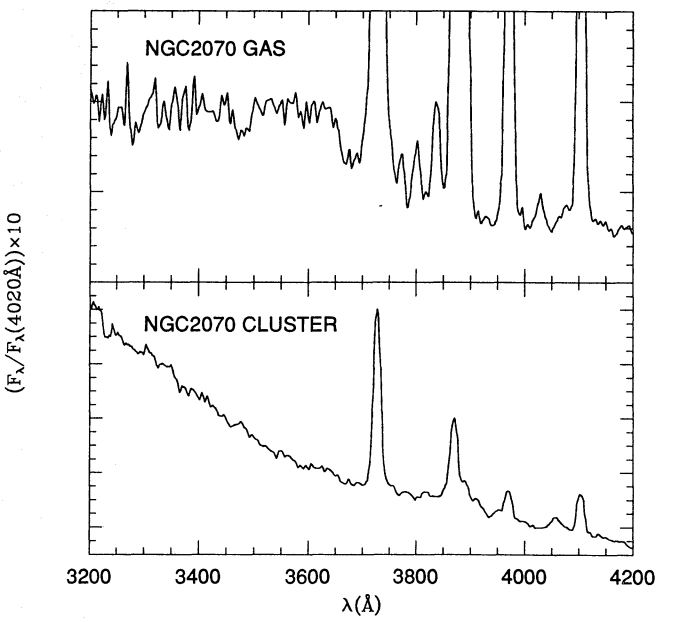

Fig. 8. Spectra of NGC2070 (30 DOR). Top: pure gas emission with the Balmer Jump in emission. Bottom: mostly stellar component, Balmer Jump is absent; some nebular emission lines are superimposed

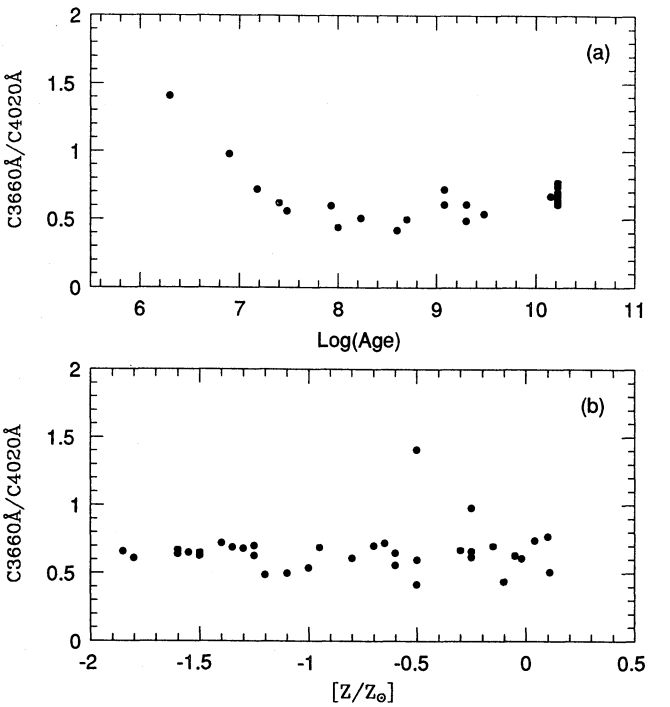

Fig. 9a and b. Balmer Jump and/or 4000Å Break as measured by the continuum ratio C3660Å/C4020Å. Top: against log(age in years). Bottom: against metallicity

Second Parameter effect (e.g. Zinn 1980). Recently, observational evidences are pointing to age differences among globular clusters as the cause of the Second Parameter phenomenon (Hesser 1992 and references therein).

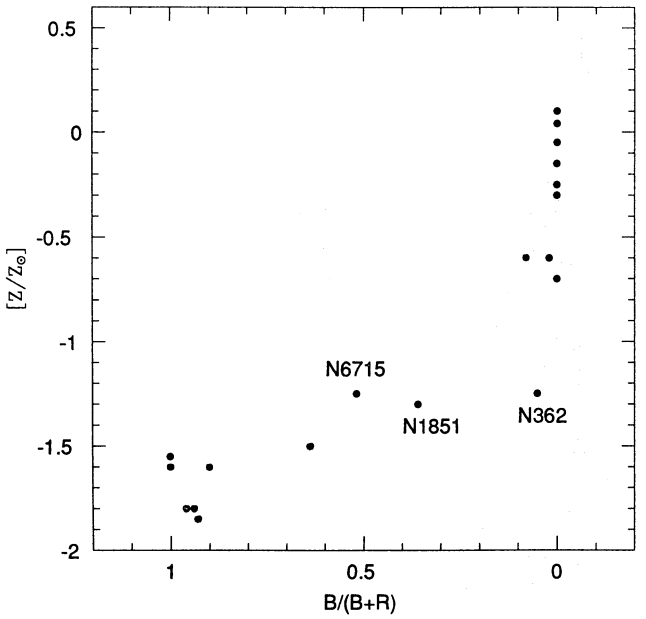

Fig. 10. Metallicity versus Horizontal Branch morphology parameter, with data from Table 1. In B/(B+R), B and R stand for the number of blue and red Horizontal Branch stars, respectively

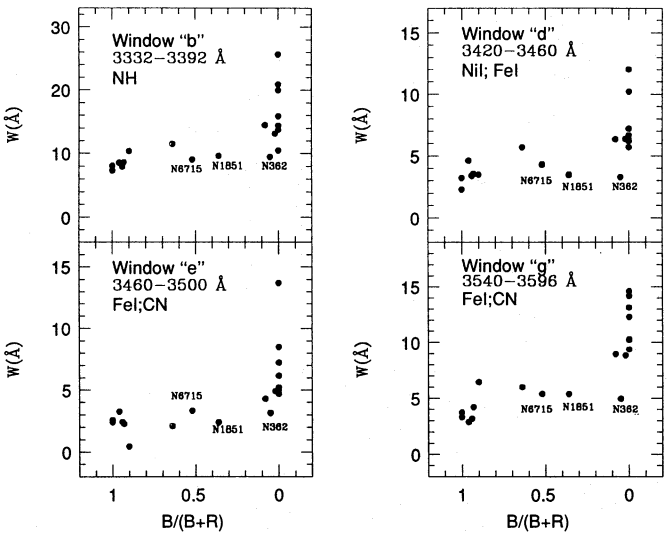

Fig. 11. Equivalent Widths of pure metallic features as a function of B/(B+R) in globular clusters

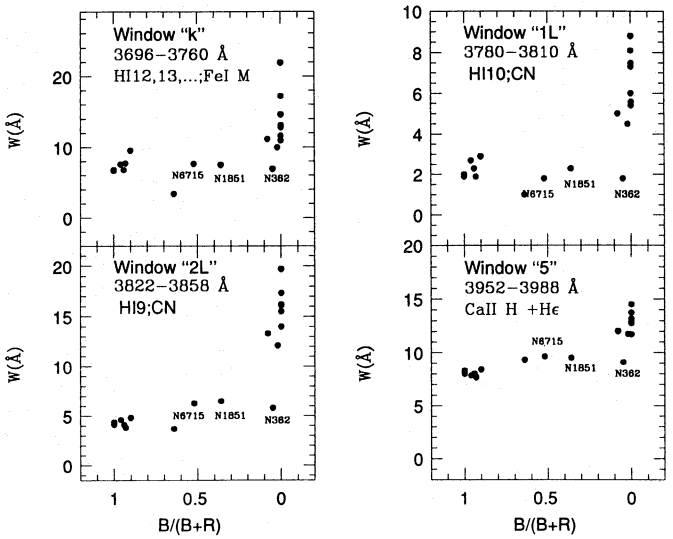

Fig. 12. Equivalent Widths for windows containing Balmer lines as a function of B/(B+R) in globular clusters.

We show in Fig. 10 the metallicity vs HB morphology (as measured by the Mironov parameter B/(B+R)), for the present sample of globular clusters with data from Table 1 (the LMC globular cluster NGC1466 is also included). The only case of a Second Parameter effect in our sample is NGC362, which has an excessively red HB morphology when compared to other clusters of similar metallicity (NGC1851 and NGC6715).

In order to study the HB morphology effects on equivalent widths we have plotted W against B/(B+R) in Figs. 11 and 12, respectively for pure metallic features and for Balmer/metal blends (the B/(B+R) counterpart of $[Z/Z_{\odot}]$ in Figs. 5 and 6). Comparing Figs. 5 and 11 we can see that the dependence of pure metallic features on B/(B+R) is less pronounced than that on $[Z/Z_{\odot}]$. As a matter of fact the Red Giant Branch, where cooler stars are present, must be contributing more than the Horizontal Branch to the integrated light. In the case of Balmer/metal blends in windows "k" and "1L" (Fig. 12) the absorption due to Balmer lines from the blue HB in the most metal poor group, becomes slightly stronger than that in clusters with intermediate B/(B+R) values. We conclude that the blue HBs in more metal poor clusters enhance the Balmer line window absorptions, but do not dilute significantly pure metallic features.

The effects of the HB morphology in terms of Second Parameter appear to be negligible, at least for NGC362, the only case in our sample. In fact the W values for these clusters are comparable, either in pure metallic or Balmer/metal blends, to those observed in normal clusters of similar metallicity NGC1851 and NGC6715 (Figs. 11 and 12). The present analysis suggests that the Second Parameter effects in stellar population synthesis of composite objects such as galaxies will be hardly detectable.

5. Concluding remarks

We present Near-UV integrated spectra of 37 star clusters in the Galaxy and in the Magellanic Clouds. They span wide age and metallicity ranges. We defined continuum tracings and a series of spectral windows for measuring feature equivalent widths. Pure metallic features in the Near-UV behave like those in the blue, except that their equivalent widths are relatively more diluted in young clusters. The continuum ratio C3660Å/C4020Å is a simultaneous measure of the Balmer Jump and the 4000Å Break. The former is an excellent age indicator for t< 50 Myr, exactly when Balmer absorption line age indicators fail. The blue Horizontal Branch in more metal poor globular clusters enhances Balmer lines, but does not dilute significantly pure

metallic features in the Near-UV, since Red Giant Branch stars appear to dominate the integrated light. From the point of view of composite population analysis, the Second Parameter effect will be almost impossible to sort out in galaxy spectra because its influence on integrated spectra of globular clusters appears to be small already.

5.1. Prospective work

The equivalent widths from the present work will be used to generate, by means of interpolations and extrapolations, a grid of star cluster properties as a function of age and metallicity. This Near-UV counterpart of the visible and Near-IR grids (BA86b and BA87) will be presented elsewhere together with an updated version of the former grid. The Near-UV spectra will also be used in building a set of templates for the visualization of population synthesis results. These cluster spectra will eventually be used to connect optical and UV data, such as the integrated star cluster spectra from IUE, with important applications to stellar population studies.

Acknowledgements. We are gratefully indebted to the ESO staff at La Silla and Garching for assistance and hospitality. D.A. in particular acknowledges the support of ESO as a visiting astronomer in august 1993, while this work was being achieved. This work was partially supported by the Brazilian institutions CNPq and FINEP. E.B. acknowledges an Assistant Astronomer position at Observatoire de Paris/Meudon (July-Sept. 1990),and H.R.S. a fellowship from CNPq. We thank Alex Schmidt for the use of the spectral analysis package SPEED.

References

Alcaino, G. 1981, A&AS, 44, 33
Alcaino, G., Liller, W., Alvarado, F. & Wenderoth, E. 1991, AJ, 102, 1371
Arp, H. & Cuffey, J. 1962, ApJ, 136, 51
Bica, E. 1988, A&A, 195, 76
Bica, E. & Alloin, D. 1986a, A&A, 162, 21
Bica, E. & Alloin, D. 1986b, A&AS, 66, 171
Bica, E. & Alloin, D. 1987, A&A, 186, 49
Bica, E. Barbuy & Ortolani, S. 1993, A&A, submitted
Boulade, O., Rose, J. A. & Vigroux, L. 1988, 96,1319
Cannon, R. D., Sagar, R. & Hawkins, M. R. S. 1990, MNRAS, 243, 151
Carbon, D. F., Barbuy, B., Kraft, R. P. et al., 1987, PASP, 99, 335
Christian, C., Heasley, J. & Janes, K. 1985, ApJ, 299, 683
Cohen, J.G., Rich, R.M. & Persson, S.E. 1984, ApJ, 285, 595
Cullum, M., Deiries, S., D'odorico, S. & Reiβ, R. 1985, A&A, 153, L1
Davidge, T. J., Robertis, M. M. & Yee, H. K. C. 1990, AJ, 100, 1143
Davis, D. N. 1947, ApJ, 106, 28
Dottori, H. A. & Bica, E. 1981, A&A, 102, 245
Faÿ, Jr. T. D., Stein, W. L. & Warren, Jr. W. H. 1974, PASP, 86, 772
Frogel, J. A. 1988, ARA&A, 26, 51
Frogel, J. A. 1992, in *"The Stellar Populations of Galaxies"*, eds. B. Barbuy , A. Renzini, Proc. IAU Symp. 149, p.245
Griffin, R. F. 1968, in *"A Photometric Atlas of the Spectrum of Arcturus"*, Cambridge Philosophical Society, Cambridge
Gunn, J. E. & Stryker, L. L. 1983, ApJS, 52, 121
Hesser, J. E. 1992, in *"The Stellar Populations of Galaxies"*, eds. B. Barbuy , A. Renzini, Proc. IAU Symp. 149, p.1
Jablonka, P., Alloin, D. & Bica, E. 1990, A&A, 235, 22
Janes, K. A. & Heasley, J. N. 1991, AJ, 101, 2097
Liller, M. H. & Carney, B. W. 1978, ApJ, 224, 383
Martins, D. H., Harvel, C. A. & Miller, D. H. 1980, AJ, 85, 529
Mould, J., Kristian, J., Nemec, J. et al., 1989, ApJ, 339, 84
Ortolani, S. Bica, E. & Barbuy, B. 1990, A&A, 236, 362
Ortolani, S. Bica, E. & Barbuy, B. 1992, A&AS, 92, 341
Ortolani, S., Bica, E. & Barbuy, B. 1993, A&A, submitted
Pagel, B. E. & Edmunds,M G. 1981, ARA&A, 19, 77
Pearse, R. W. B. & Gaydon, A. G. 1965, *"Identification of Molecular Spectra"*, Whitefrias Press Ltd., London
Richtler, T. & Nelles, B. 1983, A&A, 119, 75
Schmidt, A. A., Copetti, M. V. F., Alloin, D. & Jablonka, P. 1991, MNRAS, 249, 766
Seaton, M. J. 1979, MNRAS, 187, 73p
Shields, G. A. 1990, ARA&A, 28, 525
Stetson, P. B. 1981, AJ, 86, 687
Vallenari, A., Chiosi, C., Bertelli, G., Meylan, G. & Ortolani, S. 1992, AJ, 104, 1100
Walker, A. R. 1985, MNRAS, 217, 13P
Walker, A. R. 1992, AJ, 104, 1395
Zinn, R. 1980, ApJ, 241, 602

This article was processed by the author using Springer-Verlag TEX A&A macro package 1992.